Published in final edited form as:
Clin Cancer Res. 2011 April 1; 17(7): 2035–2043. doi:10.1158/1078-0432.CCR-10-2641.

DNA Repair Biomarker Profiling of Head & Neck Cancer: Ku80 Expression Predicts Locoregional Failure and Death Following Radiotherapy

Benjamin J. Moeller[1], **John S. Yordy**[*,1], **Michelle D. Williams**[*,2], **Uma Giri**[1], **Uma Raju**[1], **David P. Molkentine**[1], **Lauren A. Byers**[3], **John V. Heymach**[3,4], **Michael D. Story**[5], **J. Jack Lee**[6], **Erich M. Sturgis**[7], **Randal S. Weber**[7], **Adam S. Garden**[1], **K. Kian Ang**[1], and **David L. Schwartz**[1]

[1] Department of Radiation Oncology, University of Texas M.D. Anderson Cancer Center, Houston, TX

[2] Department of Pathology, University of Texas M.D. Anderson Cancer Center, Houston, TX

[3] Department of Thoracic/Head and Neck Medical Oncology, University of Texas M.D. Anderson Cancer Center, Houston, TX

[4] Department of Cancer Biology, University of Texas M.D. Anderson Cancer Center, Houston, TX

[6] Department of Biostatistics, University of Texas M.D. Anderson Cancer Center, Houston, TX

[7] Department of Head and Neck Surgery, University of Texas M.D. Anderson Cancer Center, Houston, TX

[5] Department of Radiation Oncology, University of Texas Southwestern Medical Center, Dallas, TX

Abstract

Purpose—Radiotherapy plays an integral role in the treatment of head and neck squamous cell carcinoma (HNSCC). Although proteins involved in DNA repair may predict HNSCC response to radiotherapy, none has been validated in this context. We examined whether differential expression of double-strand DNA break (DSB) repair proteins in HNSCC, the chief mediators of DNA repair following irradiation, predict for treatment outcomes.

Experimental Design—Archival HNSCC tumor specimens (n = 89) were assembled onto a tissue microarray and stained with antibodies raised against 38 biomarkers. The biomarker set was enriched for proteins involved in DSB repair, in addition to established mechanistic markers of radioresistance. Staining was correlated with treatment response and survival alongside established clinical and pathologic covariates. Results were validated in an independent intramural cohort (n = 34).

Results—Ku80, a key mediator of DSB repair, correlated most closely with clinical outcomes. Ku80 was overexpressed in half of all tumors, and its expression was independent of all other covariates examined. Ku80 overexpression was an independent predictor for both locoregional failure and mortality following radiotherapy ($P < 0.01$). The predictive power of Ku80 overexpression was confined largely to HPV-negative HNSCC, where it conferred a 9-fold greater risk of death at 2 years.

Address correspondence to: David L. Schwartz, M.D., Department of Radiation Medicine, Hofstra North Shore-LIJ School of Medicine, 270-05 76th Ave, New Hyde Park, NY 11040, Phone: 718-470-7190, Fax: 718-470-8445, Dschwartz3@NSHS.edu.
*These authors contributed equally to this work.

Conclusions—Ku80 overexpression is a common feature of HNSCC, and is a candidate DNA repair-related biomarker for radiation treatment failure and death, particularly in patients with high-risk HPV-negative disease. It is a promising, mechanistically rational biomarker to select individual HPV-negative HNSCC patients for strategies to intensify treatment.

INTRODUCTION

Radiotherapy, with or without concurrent chemotherapy, is the standard organ-preserving treatment of locally advanced HNSCC. As clinical outcomes have improved only modestly over the past several decades (1–3), treatment intensification is a focus of ongoing clinical trials. However, an inability to prospectively identify high-risk patients continues to make such efforts inefficient and exposes low-risk patients to unnecessary toxicity.

Current risk-stratification algorithms for HNSCC rely mostly on clinical data, such as AJCC stage and primary tumor subsite, which are only modestly predictive of outcomes (4,5). Mechanistic biomarkers designed to refine prospective risk-stratification have not yet been integrated into clinical practice. The emergence of human papilloma virus (HPV)-associated HNSCC as a clinically and epidemiologically distinct disease may eventually lead to tailored therapy for this subset of head and neck cancers (6–8). However, more data is needed to better understand the biology of HPV-unassociated HNSCC, since patients with this disease continue to carry the highest risks of treatment failure.

Radiation therapy, like many cytotoxic chemotherapy agents, kills tumor cells by damaging DNA. Recent work has shown that the overexpression of proteins involved in DNA damage repair, such as ERCC1, has predictive and prognostic value for various tumor types treated with chemotherapy, particularly lung cancer treated by platinum agents (9,10). Intuitively, DNA repair-related biomarkers would be particularly useful for predicting radiotherapy and chemoradiotherapy outcomes for HNSCC but none have yet been identified. Radiation causes many types of DNA damage, but the lesion contributing the most to target cell killing is the double strand break (DSB) (11). DSB repair involves a large network of proteins with complementary and redundant functions (12,13). Therefore, proper understanding of DSB phenotypes in human tumor specimens, and their relationship to disease outcomes, will require broad profiling of involved proteins. In this report, we profile the expression of 18 major DSB repair factors, as well as proteins involved in complementary signaling pathways, in a cohort of archival HNSCC specimens of known HPV infection status from irradiated patients, and correlate these profiles with disease outcomes.

MATERIALS AND METHODS

Patient Materials

All patient specimens were obtained and handled in accordance with an IRB-approved protocol (LAB09-0215). A list of all HNSCC patients treated with intensity-modulated radiotherapy (IMRT) in the Department of Radiation Oncology at the University of Texas M. D. Anderson Cancer Center was cross-referenced with the institutional Head and Neck Tissue Bank. Patients with primary tumors outside the pharyngolaryngeal axis, those without pre-radiotherapy specimens in the Tissue Bank, and those receiving induction chemotherapy were excluded.

Paraffin blocks were retrieved for all remaining patients and evaluated for inclusion on a tissue microarray (TMA). In total, 89 patient specimens were included on a TMA, which constituted the testing set. For the validation set, 74 additional patient specimens were serially sectioned for analysis. Demographic, clinical, and treatment characteristics of cases in both the testing and validation sets were typical for head and neck radiotherapy patients at

our institution: the patients were predominantly male smokers with stage IVa squamous cell carcinomas of the oropharynx, treated with radiotherapy alone (Table 1).

Local and Systemic Treatment

All patients were treated with IMRT, as described previously (14,15). IMRT was delivered using step-and-shoot multi-leaf collimation through a static treatment gantry. Treatment planning was carried out on a Pinnacle^3 system (version 6.2b or later, Philips Medical Systems, Andover, MA). Surgery and chemotherapy were employed per standard institutional clinical practice (Table 1).

Biomarker Analysis

Formalin fixed paraffin-embedded specimens were processed and stained using standard immunohistochemical (IHC) methods. Specimens were cut at 4 microns thick, mounted onto positively-charged slides, baked overnight, de-paraffinized, then boiled in 10mM citrate buffer (pH 6.0) for 20 minutes. Slides were blocked in 10% goat serum for 30 minutes at room temperature, incubated overnight with primary antibody at 4 degrees, washed, incubated with secondary antibody for 30 minutes at room temperature, washed, developed using DAB$^+$ reagent (Dako), counterstained with hematoxylin, dehydrated, and mounted under a coverslip (Supplementary Figure 1). In total, 38 biomarkers were evaluated (manufacturer and dilution details listed in Supplementary Table 1).

Two physicians (BJM and MDW) independently scored intensity (0–3+) and percentage of staining (0–100%) for each de-identified sample without knowledge of clinical data. Discrepancies between scores were rare, and were resolved by coordinated re-review of the slides between the scoring physicians. IHC scores were converted to nominal groupings (low, medium, high) according to a standardized algorithm (Supplementary Table 2).

Reverse Phase Protein Array

A total of 28 HNSCC cell lines were acquired through the M. D. Anderson Cancer Center Head and Neck cell line repository or by the American Type Culture Collection. The identity of each cell line was confirmed by DNA fingerprinting via short tandem repeat (STR) profiling (PowerPlex 1.2, Promega). HPV-negativity was confirmed by PCR (not shown). Cells were starved of FBS for 24 hours, then stimulated with 10% fetal bovine serum 30 minutes prior to the collection of whole cell protein lysate (lysis buffer: 1% Triton X-100, 50 mM HEPES pH 7.4, 150 mM NaCl, 1.5 mM MgCl2, 1 mM EGTA, 100 mM NaF, 10 mM NaPPI, 10% glycerol, 1 mM phenylmethylsulfonyl fluoride, I mM Na3VO4 and 10 ug/mL aprotinin). Protein concentrations were normalized to 1 μg/μl, and denatured at 100°C for 5 minutes in 10% 2-mercaptoethanol, 8.75% glycerol, 2% SDS, and 0.625 M Tris-HCl (pH 6.8). Duplicate samples were then serially diluted (1:2 – 1:16), transferred to 384-well plates, and printed on nitrocellulose-coated glass FAST Slides (GE Whatman) using an Aushon 2470 Arrayer (Aushon Biosystems). The microarray slides were pre-cleared with re-blot mild stripping solution (Millipore) for five minutes, then blocked for 30 minutes (I-block). Incubation with the anti-Ku80 primary antibody (Cell Signaling: 2180), secondary antibody, and secondary antibody amplification were carried out for 20, 20, and 15 minutes, respectively, with washing in TBST between each. Signal was detected using DAB chromogen for 5 minutes. Staining was captured using a CanoScan 8800 scanner with resolution set to 1200 DPI. RPPA data was quantified using SuperCurve methods (VigeneTech) and R (version 2.7.0).

Radiation Clonogenic Survival Assay

Cells cultured under ambient growth conditions were exposed to a single fraction of ionizing radiation (2 to 6 Gy) using a Mark I 137Cs irradiator (325 cGy/min, J.L. Shepherd), allowed to grow for 10 to 14 days, fixed, stained, then scored for clonogenic survival. Surviving fractions were defined by the number of clonogens surviving to form colonies of at least 50 cells, normalized to the number of cells plated, and normalized to the plating efficiency for non-irradiated cells.

Statistical Design and Data Analysis

We hypothesized that biomarkers could be found to discern an absolute survival advantage at 2 years following radiotherapy of 20% for patients with HNSCC. Based on a recent study of HPV-stratified HNSCC at the authors' institution (16), we anticipated finding a 2:1 ratio of patients with low-risk (i.e. HPV-positive) to high-risk (i.e. HPV-negative) tumors, with expected survival rates at 2 years of 95% (+/− 2.3%) and 65% (+/− 5.5%), respectively, and a combined overall 2 year mortality rate of 14% (+/− 3.6%). In order to have 80% power to confirm our hypothesis with an alpha of 0.05, 89 patient samples were needed in the testing cohort.

Based on the findings from our testing cohort, our expected event rate was revised for the validation cohort. We anticipated that Ku80 overexpression would predict an absolute survival advantage at 2 years following radiotherapy of 50%. For an unselected patient population with an expected mortality rate of 14% (+/− 3.6%), power calculations predicted that 74 samples would be needed to confirm a 20% absolute survival advantage (80% power, alpha 0.05); for a purely HPV-negative tumor cohort with an expected mortality rate of 45% (+/−4.8%), only 34 samples would be needed.

Patient demographic and clinicopathologic factors were collected, de-identified, and stored in a secured database alongside quantified immunohistochemical results. Survival rates were estimated using the Kaplan-Meier method. Comparisons between biomarker IHC staining groups (low, medium, high) were made using log-rank analysis with two degrees of freedom (SPSS version 16). Locoregional failure was defined as any persistence or recurrence of primary or regional nodal carcinoma following radiotherapy. Patients dying without evidence of locoregional failure were censored. The cumulative incidence rates of locoregional failure were calculated and compared using competing-risk methods, as previously described (17).

Frequency histograms of TMA staining scores were assembled, and comparisons between the HPV-positive and HPV–negative groups were made using Student's t-Tests, with Bonferroni corrections applied for multiple comparisons (Microsoft Excel 2007). Correlations between and amongst clinical factors and biomarkers were calculated, with significant correlations defined as those with Spearman rho coefficients greater than 0.5 (SPSS version 16). Univariate and multivariate analyses were performed based on Cox regression analyses (SPSS version 16), with IHC staining scores considered as ordinal single-level ordered variables. Unsupervised hierarchical clustering of TMA staining data was performed using average linkage clustering (Genesis version 1.7.5). Iterative processing was performed to search for the top n genes maximally discriminating survivors from non-survivors (Genesis version 1.7.5). Unless otherwise stated, significance was defined by a *P* value of less than 0.05.

RESULTS

Radiotherapy Outcome

At a median follow-up of 2 years, the locoregional control and overall survival rates for the testing cohort were 67.3 and 69.2%, respectively (Supplementary Figures 2A and C). As expected, outcomes were significantly better for patients with HPV-positive tumors compared to those with HPV-negative tumors (Supplementary Figures 2B and D).

Biomarker Distribution

We first sought to descriptively characterize the expression profiles of the biomarkers examined on this study. Frequency histograms of expression scores are shown for the entire cohort, ranked in order of increasing rate of overexpression, for DSB biomarkers (Figure 1A), and non-DSB biomarkers (Figure 1B). None of the DSB biomarkers were universally overexpressed, but most of them were overexpressed in a majority of all cases. Interestingly, several major regulators of homologous recombination – including ATM, ATR, and Rad51 – showed near-complete loss of expression in one-half to two-thirds of all cases. Expression patterns of biomarkers unrelated to DNA damage repair indicate that the majority of tumors retained an epithelial phenotype (high E-cadherin and β-catenin, low Vimentin), with a relatively low level of expression of hypoxia markers (VEGF and Osteopontin). p53 was undetectable in approximately half of all samples, and p16 was overexpressed in approximately one-third.

We confirmed HPV infection status of tumors in the testing set using a high-risk HPV genotype ISH probe set. We then stratified expression histograms by HPV status for both DSB biomarkers (Figure 1C) and DSB-unrelated biomarkers (Figure 1D). Although there was a trend towards more frequent overexpression of homologous recombination proteins in HPV-negative tumors, ATR was the only factor significantly over-represented in this cohort after correcting for multiple comparisons ($P < 0.001$). There were several significant differences in expression levels for DSB-unrelated biomarkers between HPV-positive and -negative tumors, all of which would be expected from the established biology of this virus (i.e. low p53, low pRb, high p16).

To better understand interactions occurring between the biomarkers studied, we next performed unsupervised hierarchical clustering of all derived expression profiles across the entire cohort (Supplementary Figure 3). Proteins involved in DSB repair (non-homologous end joining in red, homologous recombination in green) were tightly associated with one another, whereas biomarkers for other functional classifications were less well grouped. We also performed pairwise analyses to identify tight correlations between individual biomarkers, revealing a sizeable clustering of homologous recombination biomarkers, as well as a separate clustering of proteins affected by HPV (Figure 1E).

Ku80 as an HNSCC Biomarker

Iterative analyses of the hierarchically clustered profiles described above revealed no combination of biomarkers with significantly better predictive and prognostic value than individual biomarkers alone. Ku80 overexpression was most highly predictive of locoregional failure and death (not shown). We therefore abandoned clustering analysis in favor of linear modeling of risks of locoregional failure and death for each individual biomarker analyzed.

Univariate modeling identified overexpression of two non-homologous end joining factors – Ku80 and DNA-PKcs – as predictive of locoregional failure (Table 2). Low p16 expression levels were also predictive of locoregional failure, as would be expected, though with lower

correlation coefficients. On multivariate analysis, Ku80 was the only factor which remained predictive of locoregional treatment failure. Similar factors were also predictive of death on univariate analysis, but Ku80 and p16 remained the only markers predictive on multivariate analysis. With evidence supporting Ku80 as a predictor of both treatment failure and death, we next examined the influence of Ku80 expression levels on locoregional control and overall survival (Figure 2). High levels of Ku80 expression were significantly predictive of both local failure and death ($P < 0.005$ for each).

Since low p16 expression, a marker for HPV-unassociated disease, was also predictive of death for these patients, we next sought to separately analyze the effect of biomarker expression levels on clinical outcomes after stratifying for HPV status. Ku80 retained its predictive power on multivariate analysis for both locoregional failure and death in the HPV-negative cohort (Supplementary Table 3), but lost this predictive power for the HPV-positive cohort (Supplementary Table 4). Accordingly, Ku80 overexpression predicted for a significantly higher risk of treatment failure and death for patients with HPV-negative disease ($P < 0.05$, Figures 3A–B), but did not discriminate risk of treatment failure or death in patients with HPV-positive disease (not shown). Although there were several biomarkers predictive of treatment failure and death for patients with HPV-positive tumors by linear modeling (Supplementary Table 4), none of these ultimately predicted worse outcomes by cumulative incidence or Kaplan-Meier estimates (not shown), likely due to the low overall rate of clinical events in this patient subset.

We next sought to validate the above results in an independent cohort of patients. In light of the above results, the validation set (n = 74) was restricted to HPV-unassociated samples (n = 34), resulting in a cohort with baseline clinical and demographic characteristics similar to those of the testing population (Table 1). Locoregional control and overall survival rates for this cohort were qualitatively similar to those of the testing cohort (Figures 3C–D), showing significantly worse outcomes for patients with tumors overexpressing Ku80 ($P < 0.01$).

Finally, we used reverse phase protein array technology to profile Ku80 expression levels across 28 HPV-negative HNSCC cell lines, and correlated these values with parameters of *in vitro* radiosensitivity. The fraction of cells surviving a single dose of 2 Gy (SF2, Figure 4A), and 3.5 Gy (SF3.5, Figure 4B) correlated directly with Ku80 expression levels. Corresponding to the clinical data described above, cell lines in the upper quartile of the Ku80 expression range were six times more likely to have radiation survival fractions above the mean than below.

DISCUSSION

Preliminary results from prior studies have suggested an association between Ku protein expression and HNSCC radiation treatment outcome, but these existing data are limited by methodology and mixed findings (18–20). Our results provide strong evidence to suggest that Ku80 is a mechanistic determinant of tumor radioresistance and a biomarker for radiation treatment failure and death in patients with HPV-negative HNSCC. The ability to discriminate a 9-fold risk of death at 2 years suggests Ku80 to be a potentially valuable prognostic factor for this high-risk patient population, warranting consideration as a risk-stratification tool for future clinical trials of treatment intensification to enrich subpopulations of HPV-negative patients at highest risk for disease failure. Since Ku80 overexpression was a poor prognostic factor on this study irrespective of the use of concurrent chemotherapy, conventional platinum-based treatment intensification may not be sufficient to overcome this mechanism of radioresistance, and alternative strategies may be necessary.

There is mechanistic rationale to support an association between Ku80 expression and radioresistance. Ku80 is a key member of the non-homologous end joining (NHEJ) pathway, the principal pathway used by healthy mammalian cells to repair DSBs (21). Its relative importance is likely greater for tumor cells, where defects in alternative pathways of DSB repair – including homologous recombination – establish a greater reliance on NHEJ (22). Ku80 participates in a heterodimeric complex which forms a hollow cylinder through which the open ends of DSBs are threaded, serving as a docking station for co-factors involved in downstream enzymatic break repair. Once docked onto a DSB, the Ku heterodimer recruits DNA-PKcs, which mediates secondary signaling events required for repair (23). Experimental data directly link Ku80 with resistance to radiation (24,25) and chemotherapy (26) in preclinical models.

In light of the fact that they are functionally related, it is interesting to note that Ku80 and DNA-PKcs expression patterns were not tightly correlated in our study (Spearman coefficient < 0.5), yet both predicted for local failure and death for patients with HPV-negative HNSCC. This may reflect parallel pathways impacting Ku80 and DNA-PKcs upregulation independently. This hypothesis warrants further investigation, and serves as a potential explanation for why clinically relevant DNA repair-related biomarkers have been slow to emerge to date. Interestingly, although Ku80 was predictive for outcomes of HPV-positive disease on univariate analysis, no DNA repair related protein had prognostic value for these patients by Kaplan-Meier analysis. Given the infrequency of events in this cohort, larger sampling will be required to definitively identify potential DNA repair-related biomarkers for HPV-associated HNSCC.

A number of additional observations from our results merit emphasis. First, in contrast to earlier reports (27–30), we found no association between mesenchymal or hypoxic phenotypes and treatment resistance when analyzed in the context of our broad biomarker panel. While this may reflect limitations in patient and marker sampling, our data suggest relatively low activity in these pathways. Second, we saw no link between ERCC1 expression and treatment failure. Since chemotherapy was not the primary treatment modality used, and distant metastasis was an uncommon observation, this is not unexpected. Third, our findings establish a rationale for pursuing small molecule inhibitors of the NHEJ pathway for HPV-negative HNSCC. Moreover, the overall DSB protein profiles identified imply promising therapeutic opportunities beyond straightforward targeting of Ku80 and DNA-PKcs for radiosensitization. Attenuated expression of ATM and ATR in more than half of HNSCC tumors raises the possibility that such patients may be candidates for approaches which exploit synthetic lethality. Promotion of synthetic lethality through targeting of tumor DNA damage repair pathways has recently been validated by experimental and clinical demonstrations of efficacy of PARP inhibitors in BRCA-deficient tumors (31–33). Frequent loss of ATM and ATR may offer an opportunity to expand this paradigm into head and neck cancer.

There are limitations of the current study which deserve mention. Due to practical limitations on tumor tissue procurement, patients in our study cohort constitute a minority of the overall HNSCC radiotherapy patient population at our institution, and secondary selection biases may have been introduced during this filtering process. In addition, although we studied as broad a selection of DSB-related proteins as possible, by necessity our panel represents an abridged list. Our knowledge of DSB repair is incomplete, and of factors known to be involved, some lack reproducible antibody-based detection. Although additional DNA repair biomarkers may remain unidentified by our analysis, our methodology provided robust protein-level data for Ku80 which could be validated both in cell lines and by additional patient sampling.

In summary, our findings establish Ku80 as a candidate DNA repair-related biomarker of radioresistance and treatment failure in HNSCC. It warrants follow-up validation as a risk-stratification tool for trials designed to individualize treatment intensification. Non-homologous end joining proteins, including Ku80 and DNA-PKcs, are viable candidates for targeted inhibition for tumor radiosensitization of highest-risk HPV-negative cancer.

Supplementary Material

Refer to Web version on PubMed Central for supplementary material.

Acknowledgments

Supported by NIH P01 CA06294 and supplemented by the Gilbert H. Fletcher Memorial Distinguished Chair.

References

1. Denis F, Garaud P, Bardet E, et al. Final results of the 94-01 French Head and Neck Oncologyand Radiotherapy Group randomized trial comparing radiotherapy alone with concomitant radiochemotherapy in advanced-stage oropharynx carcinoma. J Clin Oncol. 2004; 22:69–76. [PubMed: 14657228]
2. Bonner JA, Harari PM, Giralt J, et al. Radiotherapy plus cetuximab for squamous-cell carcinoma of the head and neck. The New England journal of medicine. 2006; 354:567–78. [PubMed: 16467544]
3. Jeremic B, Shibamoto Y, Milicic B, et al. Hyperfractionated radiation therapy with or without concurrent low-dose daily cisplatin in locally advanced squamous cell carcinoma of the head and neck: a prospective randomized trial. J Clin Oncol. 2000; 18:1458–64. [PubMed: 10735893]
4. Cooper JS, Farnan NC, Asbell SO, et al. Recursive partitioning analysis of 2105 patients treated in Radiation Therapy Oncology Group studies of head and neck cancer. Cancer. 1996; 77:1905–11. [PubMed: 8646692]
5. Leon X, Gich I, Orus C, Del Prado Venegas M, Ramon Gras J, Quer M. Comparison of the Radiation Therapy Oncology Group recursive partitioning classification and Union Internationale Contre le Cancer TNM classification for patients with head and neck carcinoma. Head Neck. 2005; 27:248–57. [PubMed: 15672358]
6. Gillison ML, D'Souza G, Westra W, et al. Distinct risk factor profiles for human papillomavirus type 16-positive and human papillomavirus type 16-negative head and neck cancers. Journal of the National Cancer Institute. 2008; 100:407–20. [PubMed: 18334711]
7. Kumar B, Cordell KG, Lee JS, et al. EGFR, p16, HPV Titer, Bcl-xL and p53, Sex, and Smoking As Indicators of Response to Therapy and Survival in Oropharyngeal Cancer. J Clin Oncol. 2008
8. Ang KK, Harris J, Wheeler R, et al. Human Papillomavirus and Survival of Patients with Oropharyngeal Cancer. The New England journal of medicine.
9. Olaussen KA, Dunant A, Fouret P, et al. DNA repair by ERCC1 in non-small-cell lung cancer and cisplatin-based adjuvant chemotherapy. The New England journal of medicine. 2006; 355:983–91. [PubMed: 16957145]
10. Handra-Luca A, Hernandez J, Mountzios G, et al. Excision repair cross complementation group 1 immunohistochemical expression predicts objective response and cancer-specific survival in patients treated by Cisplatin-based induction chemotherapy for locally advanced head and neck squamous cell carcinoma. Clin Cancer Res. 2007; 13:3855–9. [PubMed: 17606717]
11. Hall, E.; Giaccia, A. Radiobiology for the radiologist. 6. Philadelphia: Lippincott Williams & Wilkins; 2006.
12. Matsuoka S, Ballif BA, Smogorzewska A, et al. ATM and ATR substrate analysis reveals extensive protein networks responsive to DNA damage. Science. 2007; 316:1160–6. [PubMed: 17525332]
13. Pan X, Ye P, Yuan DS, Wang X, Bader JS, Boeke JD. A DNA integrity network in the yeast Saccharomyces cerevisiae. Cell. 2006; 124:1069–81. [PubMed: 16487579]

14. Dabaja B, Salehpour MR, Rosen I, et al. Intensity-modulated radiation therapy (IMRT) of cancers of the head and neck: comparison of split-field and whole-field techniques. International journal of radiation oncology, biology, physics. 2005; 63:1000–5.
15. Garden AS, Morrison WH, Wong PF, et al. Disease-control rates following intensity-modulated radiation therapy for small primary oropharyngeal carcinoma. International journal of radiation oncology, biology, physics. 2007; 67:438–44.
16. Moeller BJ, Rana V, Cannon BA, et al. Prospective imaging assessment of mortality risk after head-and-neck radiotherapy. International journal of radiation oncology, biology, physics. 78:667–74.
17. Pepe MS, Mori M. Kaplan-Meier, marginal or conditional probability curves in summarizing competing risks failure time data? Stat Med. 1993; 12:737–51. [PubMed: 8516591]
18. Friesland S, Kanter-Lewensohn L, Tell R, Munck-Wikland E, Lewensohn R, Nilsson A. Expression of Ku86 confers favorable outcome of tonsillar carcinoma treated with radiotherapy. Head Neck. 2003; 25:313–21. [PubMed: 12658736]
19. Lee SW, Cho KJ, Park JH, et al. Expressions of Ku70 and DNA-PKcs as prognostic indicators of local control in nasopharyngeal carcinoma. International journal of radiation oncology, biology, physics. 2005; 62:1451–7.
20. Pavon MA, Parreno M, Leon X, et al. Ku70 predicts response and primary tumor recurrence after therapy in locally advanced head and neck cancer. Int J Cancer. 2008; 123:1068–79. [PubMed: 18546291]
21. Mahaney BL, Meek K, Lees-Miller SP. Repair of ionizing radiation-induced DNA double-strand breaks by non-homologous end-joining. Biochem J. 2009; 417:639–50. [PubMed: 19133841]
22. Powell SN, Kachnic LA. Therapeutic exploitation of tumor cell defects in homologous recombination. Anticancer Agents Med Chem. 2008; 8:448–60. [PubMed: 18473729]
23. Collis SJ, DeWeese TL, Jeggo PA, Parker AR. The life and death of DNA-PK. Oncogene. 2005; 24:949–61. [PubMed: 15592499]
24. Chang HW, Kim SY, Yi SL, et al. Expression of Ku80 correlates with sensitivities to radiation in cancer cell lines of the head and neck. Oral Oncol. 2006; 42:979–86. [PubMed: 16472552]
25. Nimura Y, Kawata T, Uzawa K, et al. Silencing Ku80 using small interfering RNA enhanced radiation sensitivity in vitro and in vivo. Int J Oncol. 2007; 30:1477–84. [PubMed: 17487369]
26. Kim SH, Kim D, Han JS, et al. Ku autoantigen affects the susceptibility to anticancer drugs. Cancer Res. 1999; 59:4012–7. [PubMed: 10463600]
27. Silva P, Slevin NJ, Sloan P, et al. Prognostic significance of tumor hypoxia inducible factor-1alpha expression for outcome after radiotherapy in oropharyngeal cancer. International journal of radiation oncology, biology, physics. 2008; 72:1551–9.
28. Le QT, Kong C, Lavori PW, et al. Expression and prognostic significance of a panel of tissue hypoxia markers in head-and-neck squamous cell carcinomas. International journal of radiation oncology, biology, physics. 2007; 69:167–75.
29. Chung CH, Parker JS, Karaca G, et al. Molecular classification of head and neck squamous cell carcinomas using patterns of gene expression. Cancer Cell. 2004; 5:489–500. [PubMed: 15144956]
30. Chung CH, Parker JS, Ely K, et al. Gene expression profiles identify epithelial-to- mesenchymal transition and activation of nuclear factor-kappaB signaling as characteristics of a high-risk head and neck squamous cell carcinoma. Cancer Res. 2006; 66:8210–8. [PubMed: 16912200]
31. Farmer H, McCabe N, Lord CJ, et al. Targeting the DNA repair defect in BRCA mutant cells as a therapeutic strategy. Nature. 2005; 434:917–21. [PubMed: 15829967]
32. Bryant HE, Schultz N, Thomas HD, et al. Specific killing of BRCA2-deficient tumours with inhibitors of poly(ADP-ribose) polymerase. Nature. 2005; 434:913–7. [PubMed: 15829966]
33. Fong PC, Boss DS, Yap TA, et al. Inhibition of poly(ADP-ribose) polymerase in tumors from BRCA mutation carriers. The New England journal of medicine. 2009; 361:123–34. [PubMed: 19553641]

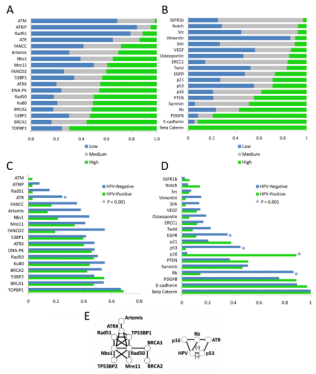

Figure 1.

Biomarker profiles. (A and B) Histograms are shown displaying the fraction of samples expressing low (blue), medium (grey), or high (green) levels of each DSB-related (A) and DSB-unrelated (B) biomarker. Markers are listed in order of increasing overexpression. (C and D) Frequency histograms showing the likelihood of overexpression (i.e. IHC score = 3) for the displayed biomarkers, stratified by tumor HPV status. Both DSB-related (C) and DSB-unrelated (D) markers are shown. Patterns varying significantly by tumor HPV status are marked with an asterisk. (E) An interactivity map is shown, with lines connecting biomarkers with highly correlated expression patterns (Spearman correlation coefficients ≥ 0.5). Two clusters are seen: an HPV cluster, and a homologous recombination cluster. All correlations are positive, except those between HPV and Rb, and HPV and p53 (−).

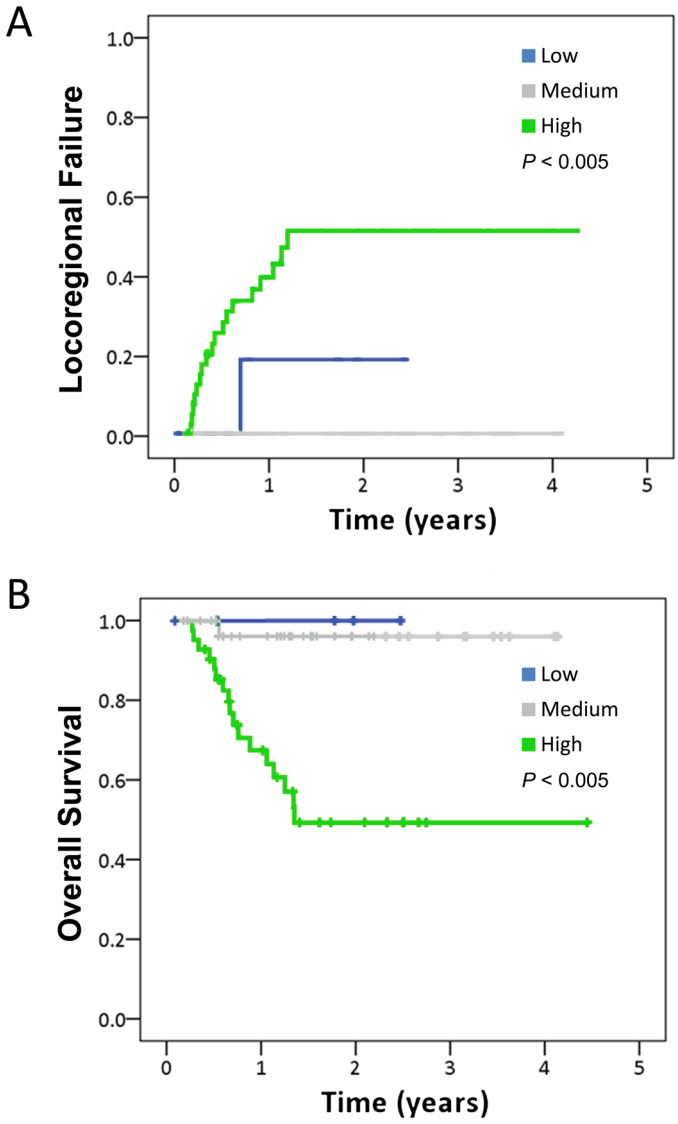

Figure 2.
Cumulative locoregional failure (A) and overall survival (B) rates for the entire testing cohort as a function of Ku80 expression score.

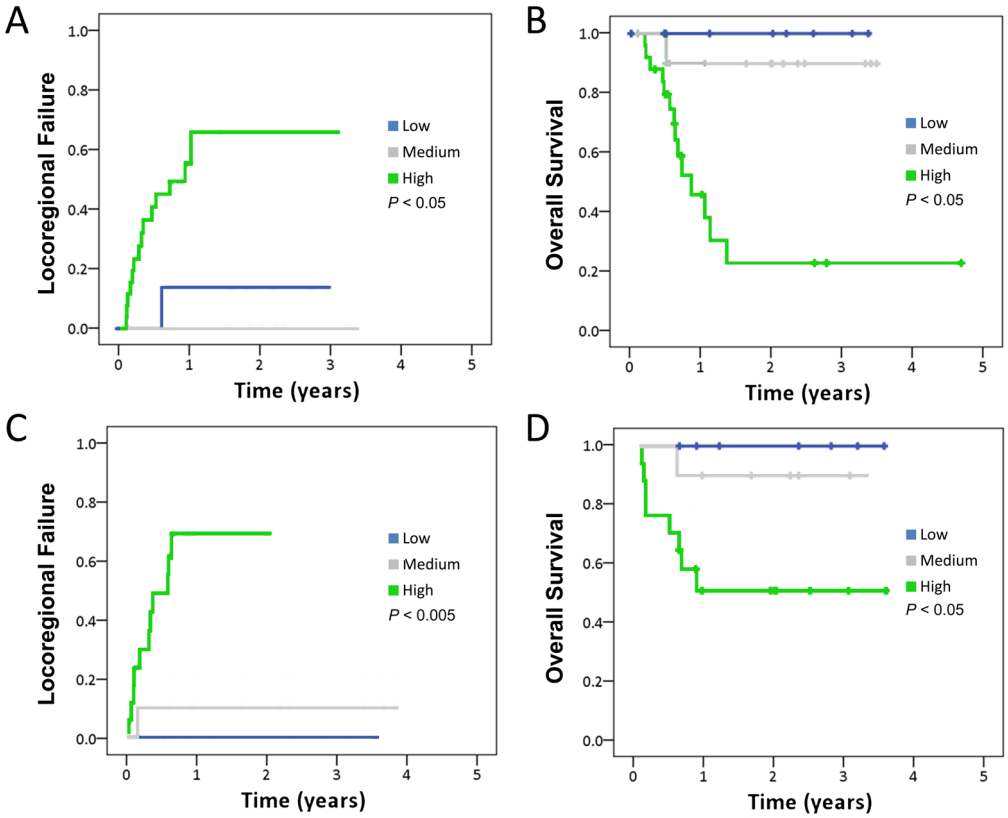

Figure 3.

Cumulative locoregional failure (A and C) and overall survival (B and D) rates for the HPV-negative subset of the testing cohort (A and B) and for the entire validation cohort (C and D) as a function of Ku80 expression score.

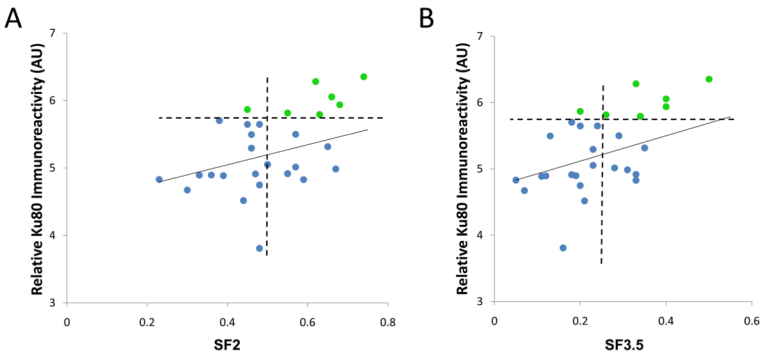

Figure 4.

For 28 individual HPV-negative HNSCC cell lines, relative Ku80 expression levels (by RPPA) are plotted against the fraction of cells surviving a single 2 Gy (A) and 3.5 Gy (B) dose of ionizing radiation. A solid line marks a linear regression through the data, showing a positive correlation between the variables. The horizontal dotted line marks the upper quartile of Ku80 expression values for the samples; the vertical dotted line marks the median SF2 and SF3.5 values. Marked in green are the cell lines falling within the upper quartile of Ku80 expression.

Table 1

Demographic, clinical, and treatment characteristics for the two patient cohorts. The number of cases or mean values for the group are provided, with percent of total or range of values in parentheses.

		Testing Set (N = 89)	Validation Set (N = 34)
Age		60 (32–84)	59 (43–81)
Sex	**Male**	73 (82)	29 (85)
	Female	16 (18)	5 (15)
Tobacco	**Yes**	57 (64)	27 (79)
	No	32 (36)	7 (21)
HPV	**Negative**	53 (60)	34 (100)
	Positive	36 (40)	0 (0)
Overall Stage	**I**	3 (3)	0 (0)
	II	12 (13)	4 (12)
	III	34 (38)	8 (24)
	IV	40 (46)	22 (64)
T Stage	**0**	4 (4)	0 (0)
	1	27 (30)	11 (32)
	2	26 (30)	7 (21)
	3	15 (17)	10 (29)
	4	17 (19)	6 (18)
N Stage	**0**	28 (31)	8 (24)
	1	8 (9)	2 (6)
	2	52 (59)	20 (58)
	3	1 (1)	4 (12)
Site	**Oropharynx**	61 (69)	23 (68)
	Larynx	21 (24)	10 (29)
	Hypopharynx	7 (7)	1 (3)
Radiation Dose (Gy)		66 (60–70)	68 (60–72)
Radiation Indication	**Definitive**	79 (89)	33 (97)
	Adjuvant	10 (11)	1 (3)
Chemotherapy	**None**	53 (60)	19 (56)
	Cisplatinum	36 (40)	15 (44)

Table 2

Linear univariate and multivariate modeling of locoregional control (LRC) and overall survival (OS) probabilities as a function of clinical and biomarker covariates for the entire testing cohort. Positive correlations imply a larger risk of failure for increasing expression values or stage. NS = not significant ($P > 0.05$). All variables listed were included in both the univariate and multivariate analyses. Other variables included in the univariate analysis that were not predictive of outcomes are not listed here; these included N stage, overall stage, radiation dose, history of tobacco use, use of chemotherapy, primary tumor location, and the remainder of the biomarkers listed in Supplemental Table 1.

Endpoint	Biomarker	Spearman's rho Coefficient	Univariate *P* value	Multivariate *P* value
LRC	**Ku80**	0.487	<0.005	**0.007**
	DNA-PKcs	0.305	0.006	NS
	p16	−0.224	0.04	NS
OS	**Ku80**	0.465	<0.005	**<0.005**
	T Stage	0.316	<0.005	NS
	HPV	−0.294	0.008	NS
	p16	−0.284	0.01	**0.02**
	DNA-PKcs	0.27	0.02	NS
	Shh	0.267	0.02	NS
	Rb	0.263	0.02	NS
	BRCA1	0.252	0.03	NS